STUDY OF GPS BASED IONOSPHERIC SCINTILLATION AND ITS EFFECTS ON DUAL FREQUENCY RECEIVER

Soumi Bhattacharya*, P.K.Purohit, Rajesh Tiwari*** and A.K.Gwal***

Abstract:

Post-sunset disturbances in the equatorial ionosphere routinely cause rapid phase and amplitude fluctuation (i.e. Scintillation) of radio waves propagating through the disturbed regions. The phenomenon of scintillations particularly in the L-band has received considerable attention in recent years because of its detrimental effects on communication and navigational systems like GPS (Global Positioning System). Amplitude scintillations induce signal fading and when the depth of fading exceeds the fade margin of a receiving system, message errors in satellite communication systems are introduced. Scintillation is not a transient phenomenon like the geomagnetic storms but is prevalent mostly during quiet periods of equinoctial months. This paper presents a study of L-band scintillations for the year 2005 from Bhopal (23.2° N, 77.6° E) which is located under the equatorial anomaly crest. A GSV4004A GPS receiver has been operational which provides the total electron content and L-band scintillation. The variations of occurrence of scintillation with time, season and magnetic activity has been discussed with the responses of dual frequency GPS receiver during severe scintillation. The result shows that very intense scintillation can degrade GPS location accuracy by limiting the number of satellites available for position fixes.

Key Words: Equatorial ionosphere, L-band scintillation, GPS, geomagnetic storms, total electron content, equatorial anomaly crest.

I. INTRODUCTION

The ionosphere is a dispersive medium, in which radio frequency signals are refracted by an amount dependent upon signal frequency and ionospheric electron density. The rapid fluctuations of the phase and intensity of a radio signal that has passed through the earth's ionosphere, typically on a satellite-to-ground propagation channel, is known as scintillation. In GPS, amplitude scintillations may cause degradation of position fixing by standalone GPS receivers [1-2], data loss and cycle slips [3]. Severe phase fluctuation may stress phase-locked loops in GPS receivers and give rise to loss of phase lock. During scintillations, In GPS,

irregular phase fluctuations are imposed on a transionospheric radio wave and amplitude fluctuations are developed by a diffraction process as the wave propagates in the free space beneath the ionosphere. Overall in the presence of scintillations, the performance of communication and navigation system is degraded. Hence in order to provide support to operational communication and navigation systems, the magnitudes of amplitude and phase scintillations and the temporal structures of scintillations need to be specified. Mainly two areas of globe particularly troubled by scintillation are sub-auroral to polar latitude and a belt surrounding the geomagnetic equator. Scintillations are most severe in the equatorial region, where they often occur after sunset, and attain maximum intensity around the peaks of the Appleton anomaly (15º N and S of magnetic equator) [4]. The electron density irregularities associated with scintillation are generated in the bottom side of post sunset F-region over the magnetic equator by the Rayleigh-Taylor instability mechanism and then rise up and align along magnetic field lines propagating to higher latitude [5]. The irregularities while diffusing along field lines break into small patches which are observed in the form of scintillations with small patch duration at low latitudes [6]. With increasing interest in understanding the behavior of ionospheric irregularities near the magnetic equator some excellent efforts have been made to examine the solar and magnetic activity control over the occurrence of scintillation associated with ionospheric irregularities [7-11].

Since ionosphere is a dispersive medium that lies on the signal path between the orbiting GPS and Satellite-Based Augmentation System (SBAS) satellites and the users, the ionosphere refracts the broadcast RF wave by an amount proportional to the total electron content (TEC) along its path and as a function of the signal frequency. With the advent of the GPS based navigation, there is a renewed interest in scintillation studies. It is because the scintillation not only degrades the received signal, the plasma density variations associated with the scintillation, that manifest as variations in the total electron content (TEC), introduce large range errors. It is well known that ionospheric scintillation has the potential to affect all types of GPS receivers and the most severe natural scintillation in the world occurs in the nighttime equatorial ionosphere. Therefore, it is desirable to obtain further understanding of ionospheric scintillation and its effects on GPS by means of a receiver capable of performing its operations in such conditions. So to monitor this region the GISTM receivers were deployed at a number of low latitude sites and functioned well through the mid-nineties, a period of low solar activity. To investigate equatorial scintillation dynamics and evaluate the performance of GPS receiver during scintillation period, the preliminary results are presented here for scintillation impacts on GPS communication and navigation.

* *Space Science Laboratory, Barkatulla University, Bhopal ; e-mail: sbhattacharya_82@yahoo.co.in*

** *National Institute of Technical, Teacher Training and Research, Shamla Hills, Bhopal-462026, India*

*** *Calgary University, Calgari, Canada*

II. IONOSPHERIC SCINTILLATION MONITORING AND METHODOLOGY

Using a GPS ionospheric scintillation and TEC monitoring (GISTM) dual frequency L1 (1575.42MHz) and L2 (1227.60MHz) receiver, data were recorded at Space Science Laboratory, Department of Physics, Barkatullah University, Bhopal (lat. 23.2º N, long.77.6º E). The data analyzed and discussed in this paper used from January 2005 to December 2005. This receiver provides total electron content (TEC) as well as the measurements of amplitude and phase scintillations in the forms of S_4 and σΔΦ, updated at one-minute intervals at a 50-Hz rate and code/carrier divergence at a 1-Hz rate. During the observed scintillation, the receiver records the lock-time which is defined as the time required for the receiver to lock onto a satellite and carrier-to-noise ratio (C/No). For the data to be useful the receiver must maintain lock for more than 240 seconds. This is the time required for the detrending HPF (High Pass Filter) to re-initialize lock with the carrier phase signal. If the receiver loses lock on a satellite for less than 240 seconds unrealistic high phase values are present (greater than expected for scintillation) and so the phase data is ignored.

Amplitude Scintillation

Amplitude Scintillation is obtained by monitoring the index S_4. The S_4 index is derived from detrended signal intensity of signals received from satellites Van Dierendonck et al [12]. The S_4 index, which includes the effects due to ambient noise, is defined as the normalized root mean square of the power P divided by the average power P as follows:

$$S_{4T} = \sqrt{\frac{\langle P^2 \rangle - \langle P \rangle^2}{\langle P^2 \rangle^2}} \qquad (1)$$

where ⟨⟩ represents the average values over a 60-second interval.

Removing the Effects of Ambient Noise

The Total S_4 defined in equation 1 has a significant amount of ambient noise associated with it, which needs to be removed before further analysis. This is achieved by estimating the average signal-to-noise density (S/N_o) over a 60-second interval. This estimate is then used to determine the expected S_4 due to ambient noise (also known as S_4 correction) as follows:

$$S_{4N_0} = \sqrt{\frac{100}{S/N_0}\left[1 + \frac{500}{19S/N_0}\right]}$$

Replacing the S/N_o with the 60-second estimate, S/N_o, gives the S_4 due to noise. Hence, subtraction of equation (1) and (2) yields equation (3), which is the S_4 with the effect of ambient noise removed.

$$S_4 = \sqrt{\frac{\langle P^2 \rangle - \langle P \rangle^2}{\langle P \rangle^2} - \frac{100}{S/N_0}\left[1 + \frac{500}{19S/N_0}\right]}$$

Phase Scintillation

Phase measurements are obtained by monitoring the standard deviation, σ?Φ, and the power spectral density of the detrended carrier phase from signal received satellites. The spectral slope is measured above 1 Hz from detrended carrier and the spectral strength is measured at 1 Hz from detrended carrier. The detrending of the carrier phase is achieved by passing the raw 50 Hz phase measurements through a sixth-order high-pass Butterworth filter. This removes all the low frequency effects below its cut-off of 0.1 Hz Van Dierendonck et al [13]. The σ?Φ's are computed over 1, 3, 10, 30 and 60 second intervals at every 60 seconds using the 50 Hz detrended phase measurements. The 1, 3, 10, 30 and 60 seconds σ?Φ's are further averaged over the 60-second interval.

Total Electron Content

The electron density is obtained by summing the number of electrons in a vertical column with a cross-sectional area of 1 m^2, extending from the GPS satellite to the receiver. The electron density thus obtained is termed as the Total Electron Content (TEC) Klobuchar, [14] and is mathematically expressed as:

$$TEC = \int_p N\, ds \quad (4)$$

where N is the electron density m^{-3} and p is the propagation path between the satellite and the detector. A TEC unit is defined as 1×10^{16} electrons m^{-2}. TEC measurements are generally derived from satellite radio signals observed at various angles, and are normally expressed as an equivalent vertical TEC by dividing the slant TEC by the secant of the elevation angle at a mean ionospheric height (i.e., 350 – 400 km). Here, vertical TEC is used, as it is more easily comparable than slant values at various angles. A different scale of ionospheric irregularities can be described by using the distributive variation of the Ionospheric TEC, which can be retrieved from a GPS signal. Monitoring the time-derivative of TEC (ROT, rate of change of TEC) is useful for tracing the presence of irregularities. Equation (5) shows the algorithm to calculate ROT [15].

$$ROT = \frac{TEC^{\,i}_{k} - TEC^{\,i}_{k-1}}{(t_k - t_{k-1})}$$

where *i* is the visible satellite and *k* is the time of epoch.

The observations of amplitude scintillation for the year 2005 are described in this paper. Statistical calculations were further limited to those measurements made from satellite with elevation angle greater than 30° to limit multipath interference. The parameters adopted at this work are: $S_4 \geqslant 0.05$ and $S_4 \leqslant 0.2$ for very weak scintillation; $S_4 \geqslant 0.2$ and $S_4 \leqslant 0.4$ for weak scintillation; $S_4 > 0.4$ and $S_4 \leqslant 0.6$ for moderate scintillation; and $S_4 > 0.6$ for strong scintillation. In this analysis, we consider only data with S_4 larger than 0.2. The average annual variations of scintillation occurrences (%) for the year 2005 are shown in fig 1. In this case the percentage of

occurrence is computed by the ratio between the total number of observations of each month with scintillation (S_4>0.2) to the total number of observations during the whole year with scintillation and the time of epoch was 0000-2400 hrs LT. This is the mostly used method to study the occurrence of ionospheric irregularities causing scintillations in the GPS satellite signals [16-17]. It is observed from the Fig.1 that the scintillation occurrence is maximum in March and January while minimum in November and May. This figure also reveals that maximum scintillation occurrence was below 0.2 along the year which shows that much weak scintillations affect the GPS satellites signals at equatorial latitudes. Once the electron density is lower close to the dip equator and also due to the absence of turbulences at the Fresnel length the scintillations at L-band frequencies are weak in the magnetic equator. The equinoxial maxima are explained on the basis of the alignment of the solar terminator with the magnetic meridian in both the hemispheres [18]. Over the sunlit hemisphere, the E-region ionization short circuits the polarization electric fields developed in the F-region during the evolution phase of the ESF irregularities. During the equinox, the solar terminator aligns closely with the magnetic meridian, thereby simultaneously decreasing the conductivity of the E-regions that are magnetically conjugate to the F-layer, through which currents flowing along the geomagnetic field lines connect the F-region to the E-regions on either side of the equator (which acts as a short circuit over the sunlit hemisphere). This alignment causes the decrease in E-region conductivity, which opens or releases the F-region dynamo electric field, which, in turn, produces the ***E*×*B*** upward drift of the equatorial F-layer, creating favorable conditions for the generation of plasma irregularities during the equinox months, as seen from the figure 1 & 2.

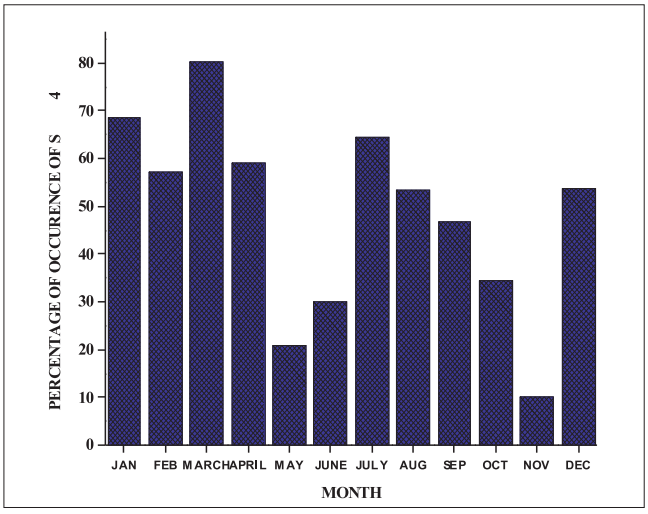

Fig1. *Annual variation of percentage occurrence s cintillation for the year 2005*

Seasonal variation of scintillations

To study the nocturnal variations of percentage occurrence of scintillations for the three seasons, we grouped all the months in three categories corresponding to Equinox, Winter and Summer. Figure2. shows a remarkable seasonal variation. It shows that scintillation activity is maximum during equinox months while minimum in summer months. In case of seasonal variation, percentage occurrence of scintillations is maximum in pre-midnight hours and minimum in post midnight hours during equinox and winter months while in summer months the maximum occurrence of scintillation is in the post-midnight hours and minimum in pre-midnight hours. As reported by Makela et al.[19], post midnight extension of GPS scintillations are due to the overall increase in the ionospheric electron density.

The most basic potential source to generate the post sunset ionospheric plasma irregularities is the evening uplift of the F-layer at equatorial latitudes, produced by an enhancement in the zonal (eastward) electric field, widely called as the pre-reversal enhancement (PRE). Therefore, such increase in the PRE could be a basic requirement to explain an increase in the GPS scintillation activity from one season to another. The stronger the evening PRE the higher is the plasma density at higher altitudes in the equatorial F-region and, consequently, more large density deviations (*?N*) might occur at that height. Once the scintillation depends strongly on the electron density fluctuations (*?N*) [20], larger *?N* could be a significant source for higher scintillation occurrence to be observed at equinoctial and winter months. A good number of workers have studied the effect of seasonal variation of scintillations for many years at equatorial and low latitudes and had the same results [21, 22, 7,8, 10].

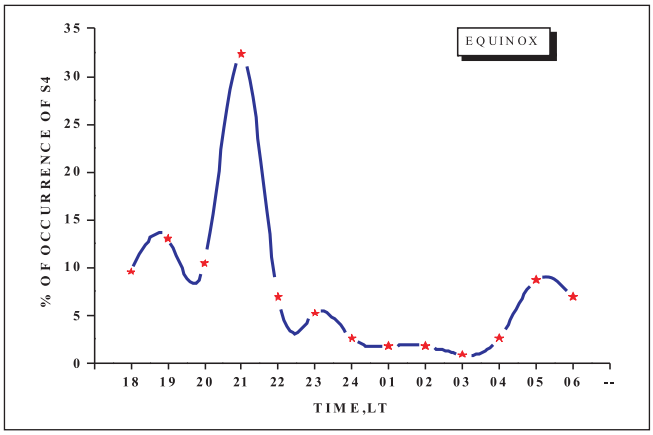

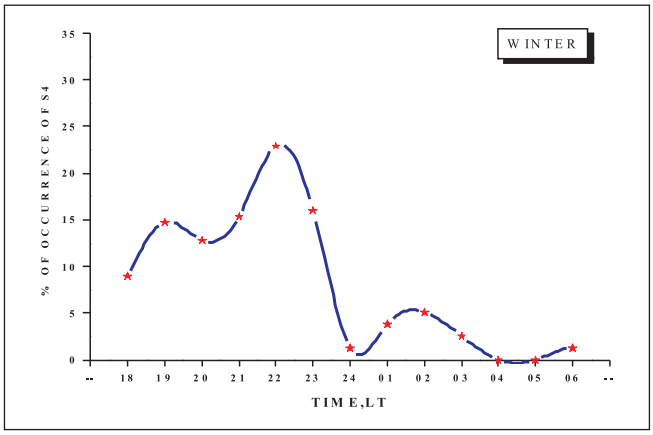

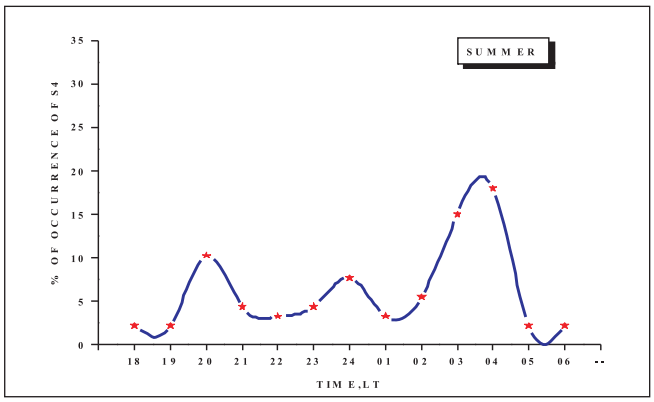

Fig 2. *Nocturnal variation of the percentage occurrence of amplitude scintillations for three different seasons*

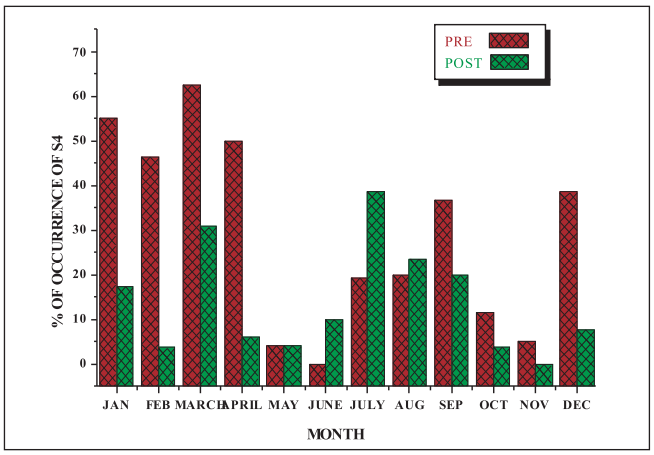

Fig 3. *Monthly percentage occurrence of amplitude scintillations during pre-midnight and post-midnight*

Figure 3 shows the monthly mean percentage of occurrence of scintillation during pre-midnight (1800-2400 hrs LT) and post-midnight (2400-0600 hrs LT) period for each month. It is seen that pre-midnight occurrence of scintillation was predominant in most of the months except in the month of June, July and August, when post-midnight scintillation was predominant. Pre-midnight scintillation was found to be maximum in March while post-midnight scintillation maximized in July. May showed same duration of pre-midnight and post-midnight scintillation.

During the pre-sunset period, the eastward electric field is increased, causing an increase in F-layer height [23]. A negative excursion of ring current during this period would lower the local eastward electric field and reduce the F-layer height. This effect may sometimes be large enough to reverse the upward movement of F-layer during the post-sunset period, thereby inhibiting the creation of irregularities. This may result in a suppression of pre-midnight scintillations over most longitudes during periods of intense magnetic activity. However, scintillations may continue to appear at some longitudes. At midnight and during the post-midnight period when the electric field is westward and the F-layer height is falling, the ring current may create a short-lived eastward electric field. This may cause the F-layer height to rise momentarily before failing again. Such a situation may create irregularities and this might be the cause of scintlllations during premidnight and post midnight periods. Sastri et al. [24] have suggested that even in the presence of favorable conditions, like an eastward electric field, some as yet unidentifiable factors may suppress the generation of fresh irregularities in the post-midnight period. Using the measurements of thermospheric neutral wind and irregularities drift, Valladares et al. [25] have investigated the coupling between ions and neutrals at the equatorial latitudes. They have related the variability of this coupling to the occurrence of scintillations.

Scintillation occurrence and the satellite elevation angle

To study the occurrence of equatorial scintillations at Bhopal we used the S_4 index greater than 0.2. The 0.2 threshold for the S_4 index can be considered to be above the level of noise and multipath effects. On the other hand, it cannot be true for satellites tracked at low elevation viewing angles. For many purposes, it is acceptable to use GPS satellites above 30º of elevation angle to minimize effects of geometric factors in the S_4 index calculation. To minimize any external influence that may biases our results we used only satellites with elevation angles above 30º. This angle mask reduces the variations of the ionospheric distances at the scattering height due to the satellite movement and ensures that only the local ionosphere over the observation site is being sampled [26]. Figure 4 shows the percentage of GPS satellites whose signals are scintillating at different elevation angles. It is calculated from the ratio between the numbers of scintillating GPS satellites tracked above 30º, 45º, 60º or 75º, by the total number of observations computed during the entire nights throughout January 2005 to December 2005. It can be seen from the figure that the number of affected GPS satellites reduces significantly from ~43% to ~8% when the elevation mask increases from 30º to 45º. It happens mainly because the number of satellites available at higher elevation angles decreases. Otherwise, we cannot neglect other important factors such as the lower the elevation angle the weaker is the received signal and consequently, larger can be the S_4 index value than that physically expected. Normally, the number of satellites available above 45º is one to four, but for elevation mask of 60º it reduces from zero to three at most of the time. The IPP is the parameter that represents the assumed altitude of the centroid of the mass of the ionosphere [27], which is mostly used in the calculation of converting the measured slant TEC into vertical TEC (VTEC). Recently, Rama Rao et al. [28] have shown, for the Indian sector, how sensitive is the value of TEC when used data from satellite passes with elevation angles lower than 50º. They reported that an IPP of 350 km may not be valid when GPS satellites with elevation angles lower than 50º are used for regions where the spatial and temporal variation of TEC are significant. This is also what happens over the Bhopal region, where the ionosphere covers the magnetic equator. Moreover, the use of high

satellite elevation angles is the most appropriated to study simultaneous co-existence of scintillations with the plasma bubbles signatures obtained from different techniques of measurements.

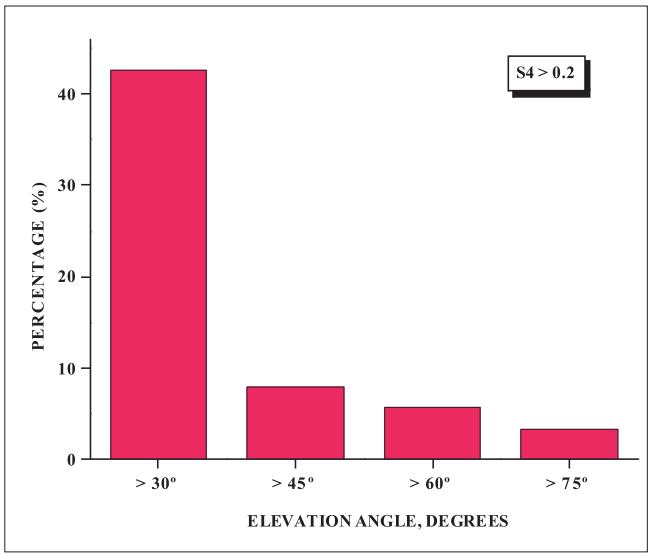

Fig 4. *Percentage occurrence of amplitude scintillations with elevation angles during 2005*

Effect of Magnetic Storm

The role of magnetic storm associated with the occurrence of L-band scintillation at Bhopal is examined. The planetary magnetic activity indices Kp, the Dst values, Bz-component of the IMF, auroral indices AU and AL and the occurrence time of scintillation activity during 21-January 2005 storm are the sources of our study. Figure 5 shows Kp, Dst and IMF-Bz plots in the three upper panels. Fourth panel shows the AU & AL indices and last panel shows the scintillation occurrence with time. Dst value shows minima at 2200 UT with -99 nT on 21 January 2005. The Kp values shows a maximum of 7. According to Aarons [29] this was a Category 1 storm. We can see from the figure that only on 22 January 2005, there was no observed scintillation activity. During the event, the Bz-IMF was strongly positive with 12 nT and a quiet recovery phase of the ring current without additional injections was observed on the Dst-plot. After 1800 UT, the main phase of the storm started with increasing AL (776 nT) and AU but later at 2000 UT AU starts decreasing and reaches its value with 368 nT. It should be noted that the auroral electrojet has a faster recovery phase than the ring current, as one can see from the AL and Dst plots. Thus, conditions for the generation of scintillation activity during the storm recovery phase were not satisfied at this sector of the equatorial ionosphere. The example considered indicates that there can be different causes for generation or inhibition of the equatorial scintillations. Iigima and Potemra [30], showed that the location and intensity of the field-aligned currents (FAC) are determined by the Bz and By components of the IMF. According to the model of Sizova and Pudovkin [31], electric field of the field-aligned currents penetrates through the mid-latitudes to the low-latitude ionosphere and creates the additional equatorial electric fields. These electric fields modify the equatorial electrojet and the ionospheric plasma vertical drift velocity. If the Bz IMF is negative, the equatorial electrojet is enhanced by the FAC and plasma moves upward away from the F-layer. In this case a maximum of the F2-layer is observed at the high altitudes where irregularities are observed. Therefore, the FAC are in the continuous dynamics, thereby becoming responsible for the complicated nature of height variations at the equator. During the positive Bz IMF the F-layer cannot rise up 350km for the generation of scintillations. As shown by Burton et al. [32], Sizova and Zaitseva [33]. Pudovkin et al. [34] the magnetospheric ring current intensity is strongly dependent on the variations of the Bz IMF. The magnetospheric ring current cannot directly penetrate to the equatorial ionosphere, though these are models with closed partial ring current through the polar ionosphere [35]. According to the model of Sizova and Pudovkin [31], electric fields of the field aligned currents penetrate through the mid-latitude to the low latitude ionosphere and create the additional equatorial electric fields. Under the additional eastward electric field, the height of the F-region rises high enough where scintillation irregularities can be generated. The generation or inhibition of irregularities during the main phase/recovery phase of a magnetic storm depends upon the location of the station and local time. The inhibition and generation of irregularities during enhanced magnetic activity period are explained by considering changes in the electric field. The role of the storm time electric

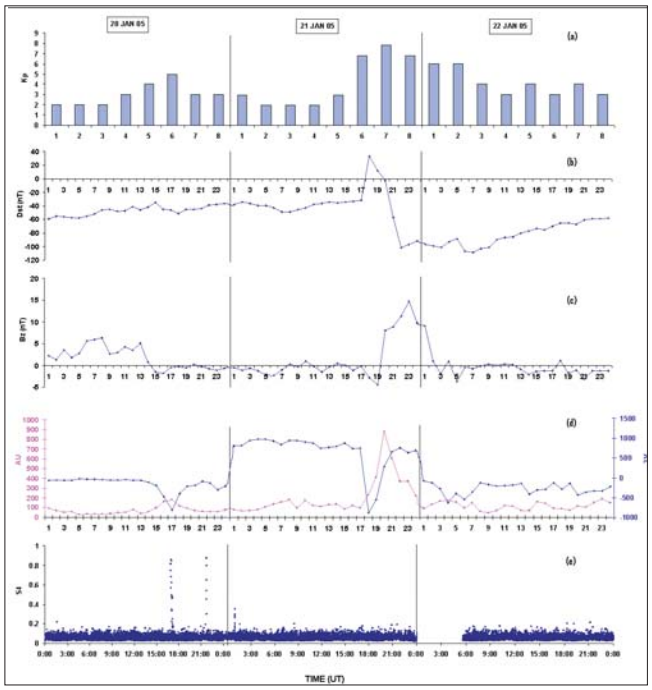

Fig. 5 *: Scintillation associated with magnetic storm of 21-January 2005. The upper three panels shows the Kp, Dst and IMF Bz indices and fourth panel shows the AU & AL indices.*

field is very complex. It appears that the magnetospheric electric field changes related to the ring current intensification are not sufficient to explain all of the observations of inhibition and the generation of low latitude ionospheric irregularities during the night. Apart from the ring current, there are several other factors which shape the development of irregularities, such as the ion-neutral collision frequency, neutral wind, large scale plasma density gradient, gravity wave etc. A magnetic storm enhances the interplay of these parameters and hence their contributions should be considered separately.

IV. CONCLUSION

This paper presents a study of equatorial scintillations particularly at L-band from GPS satellites observed at Bhopal. Bhopal is located near the crest of the equatorial anomaly and severe scintillation on L-band are frequently observed at this station in the pre sun-set hours of equinoctial months. The percentage occurrence of weak (S_4>0.2) scintillations is maximum at the equatorial region, owing to the presence of low ambient electron densities and low gradients accompanied by the presence of large-scale length irregularities at the equator during the low solar activity conditions in the year 2005. In this paper we also presented our initial approach to correlating scintillation data with the TEC behavior given by dual-frequency data and to monitor the number of losses of lock of the L1 signal with C/No. on an operational basis that provides an indication of the level of influence of scintillation activity on GPS. The occurrence of strong scintillations is mostly confined to 15º to 25º N geographic latitudes i.e. 5º to 15º N geomagnetic latitudes in the Indian region. Result shows that intense equatorial scintillations may disable satellite-based communication and navigation systems like GPS and SBAS for a considerable period of time resulting in position errors and loss of data. The statistical study of the fading amplitude and duration is very important to design GPS receivers more robust to ionospheric scintillation and this study also for solar minimum conditions is been performed.

REFERENCES

1. Bandyopadhyay T, Guha A, DasGupta A, Banerjee P & Bose A, Degradation of navigational accuracy with Global Positioning System during periods of scintillation at equatorial latitudes, *Elect. Lett.,* 33, 1010-1011, 1997.
2. DasGupta A, Ray S, Paul A, Banerjee P & Bose A, Errors in position fixing by GPS in an environment of strong equatorial scintillations in the Indian zone, *Radio Sci. (USA),* 39, RSIS30, doi: 10.1029/2002RS002822, 2004.
3. Kelley M C, Kotsikopoulos D, Beach T, Hysell D & Musman S, Simultaneous Global Positioning System and radar observations of *equatorial spread F at Kwajalein, J. Geophys. Res.(USA),101, 2333-2341, 1996.*
4. Basu S, MacKenzie E & Basu Su, Ionospheric constraints on VHF/UHF communications links during solar maximum and minimum periods, *Radio Sci. (USA),* 23, 363-378, 1988.
5. Kelley M C, The Earth's Ionosphere, *Academic*, San Diago, CA, 1989.
6. Singh R P, Singh A K, Singh U P, Singh R N, Scintillation Study at Varanasi, *Indian Journal of Radio & Space Physics*, 22, 17-21, 1993.
7. Kumar S & Gwal A K, VHF ionospheric scintillations near the equatorial anomaly crest: solar and magnetic activity effects, *J. Atmos. Sol. Terres. Phys.(UK)*, 62, 157-169, 2000.
8. Singh R P, Patel R P & Singh A K, Effect of solar and magnetic activity on VHF scintillations near the equatorial anomaly crest, *Annales Gepphysicae*, 22, 2849-2860, 2004.
9. Biktash L Z, Role of magnetospheric and ionospheric currents in the generation of the equatorial scintillations during geomagnetic storm, *Annales Geophysicae,* 22, 3195-3202, 2004.
10. Dubey S, Wahi R, Mingkhwan E & Gwal A K, Study of amplitude and phase scintillation at GPS frequency, *Ind. J. Rad. Spa..Phys,* 34, 402-407, 2005.
11. Li G, Ning B, Wan W & Zhao B, Observations of GPS Ionospheric scintillations over Wuhan during geomagnetic storms, *Annales Gepphysicae,* 24, 1581-1590, 2006
12. Van Dierendonck A J, Klobuchar J & Quyen Hua, Ionospheric Scintillation Monitoring Using Commercial Single Frequency C/A Code Receivers, *Proceedings of ION GPS-93, Salt Lake City, UT, September 1993.*
13. Van Dierendonck A J, Pat Fenton & Klobuchar J, Commercial Ionospheric Scintillation Monitoring Receiver Development and Test Results, *Proceedings of ION 52nd Annual Meeting. Cambridge, MA., June 19-21, 1996.*
14. Klobuchar J A, Ionospheric effects on GPS, *GPS World, April 1991.*
15. Pi X, Mannucci AJ, Lindqwister UJ, Ho CM, Monitoring of global ionospheric irregularities using the worldwide GPS network, *Geophys. Res. Let*, 24, 2283-86, 1997.
16. Gwal A K, Dubey S & Wahi R, A study of L-band scintillations at equatorial latitudes, *Adv Space res,* 9, 2092-2095, 2004.
17. de Paula E R, Kherani E A, Abdu M A, Batista I S, Sobral J H A, Kantor I J, Takahashi H, de Rezende L F C, Muella M T A H, Rodrigues F S, Kinter P M, Ledvina B M, Mitchell C N & Groves K M, Characteristics of the ionospheric F-region plasma irregularities over Brazilian longitudinal sector, *Ind J Rad Spa Phys* 36, 268-277, 2007.
18. Tsunoda R T, Control of the seasonal and longitudinal occurrence of equatorial scintillations by longitudinal gradient in the integrated E-region Paderson conductivity, *J. Geophys. Res.* 90, 47–456, 1985.

19. Makela J J, Ledvina B M, Kelly M C & Kintner P M, Analysis of the seasonal variations of equatorial plasma bubble occurrence observed from Haleakala, Hawaii, *Ann. Geophys.* 22*,* 3109-3121, 2004.

20. Yeh K C & Lic C H, Radio wave scintillations in the ionosphere, *Proc IEEE* 70, 324-360, 1982.

21. Kumar S, Vijay S K & Gwal A K, "Some results of night-time scintillations at low latitude", *Proc. Indian Acad. Sci. (Earth Planet. Sci.)(Japan),* 102, No.2, June, 307-312, 1993.

22. Rama Rao P V S, Tulasi Ram S, Niranjan K, Prasad D S V V D, Gopi Krishna S & Lakshmi N K M, VHF and L-band scintillation characteristics over an Indian low latitude station, Waltair (17.7º N, 83.3º E), *Annales Geophysicae*, 23, 2457–2464, 2005.

23. Fejer B G, Scherliess L & dePaula E R, Effects of the vertical plasma drift velocity on the generation and evolution of equatorial spread F, *J. Geophys. Res. (USA),* 104, 19859-19869, 1999.

24. Sastri J H, Jyoti N, Somayajulu V V, Chandra H, & Devasia C V, Ionospheric storm of early November 1993 in the Indian equatorial region, *J. Geophys. Res. (USA),* 105, 18 443–18 455, 2000.

25. Valladares C E, Meriwether J W, Sheehan R, & Biondi M A, Correlative study of neutral winds and scintillation drifts measured near the magnetic equator, *J. Geophys. Res.* 107 (A7), 2002.

26. Kil H, Kintner P M, de Paula E R, Kantor I J, Global Positioning system measurements of the Ionospheric zonal apparent velocity at Cachoeira Paulista in Brazil, *J. Geophys Res.* 105*,* 5317-5327, 2000.

27. Birch M J, Hargreaves J K, Bailey G J, On the use of an effective Ionospheric height in electron content measurement by GPS reception, *Radio Sci,* 37*,* doi: 10.1029/2000RS002601, 1-19, 2002.

28. Rama Rao P V S, Niranjan K, Prasad D S V V D, Gopi Krishna S, Uma G, On the validity of the ionospheric pierce point (IPP) altitude of 350 km in the Indian equatorial and low latitude sector, *Ann. Geophys.* 24, 2159-2168, 2006.

29. Aarons J, The role of the ring current in the generation or inhibition of equatorial F-layer irregularities during magnetic storms, *Radio Sci,* 26, 1131-1149, 1991.

30. Iigima T, & Potemra T A, Large scale characteristics of the field aligned currents associated with substorms, *J. Geophys. Res. 83,* 599-615, 1978.

31. Sizova L Z & Pudovkin M I, Disturbances of the daytime equatorial ionosphere associated with the Bz-component of interplanetary magnetic field, *Geomagn. Aeron* 40, 246-249, 2000.

32. Burton R K, McPherron R L, & Russel C T, An empirical relationship between interplanetary conditions and Dst, *J. Geophys. Res. 80*, 4204-4241, 1975.

33. Sizova L Z & Zaitseva S A, The growth rate and decay of magnetospheric ring current, *Moscow Preprint IZMIRAN* 52*,* 1-23, 1984.

34. Pudovkin M I, Zaitseva S A, & Sizova L Z, Growth rate and decay of magnetospheric ring current, *Planet Space Sci* 33, 1097-1102, 1985.

35. Kikuchi T, Luhr H, Kitamura T, Saka O & Schlegel K, Direct penetration of the polar electric field to the equator during a DP event as detected by the auroral and equatorial magnetometer chains and the EISCAT radar, *J. Geophys. Res. 101*, 17161-17173, 1996.

n